

Characteristics of Mononuclear Ruthenium–Oxo Complexes Adjusted by Axial Ligand for the Catalysis of Oxygen-Transfer Reactions

Takeshi Okumura, Yuji Morishima, Hiroyoshi Shiozaki, Takeyoshi Yagyu, Yasuhiro Funahashi, Tomohiro Ozawa, Koichiro Jitsukawa,* and Hideki Masuda

Department of Materials Science and Engineering, Graduate School of Engineering, Nagoya Institute of Technology, Showa-ku, Nagoya 466-8555

Received July 14, 2006; E-mail: jitsukawa.koichiro@nitech.ac.jp

Ruthenium(II) complexes, [Ru(babp)(dmso)L], consisting of tetradentate square-planar ligand (babp = 6,6′-bis-(benzoylamino)-2,2′-bipyridinato) and two monodentate axial ones, DMSO and L (L = dmso or heterocycles), were synthesized and structurally characterized using UV–vis, NMR, ESI-MS, and IR spectroscopies and X-ray crystallography. These complexes showed catalytic activity toward the oxygen-atom-transfer reactions, such as epoxidation, allylic oxidation, cleavage reaction of olefins, and sulfoxidation of thioethers, in the presence of oxidant, PhIO. The relationship between the coordination structure and the catalytic activities of [Ru(babp)(dmso)L] was investigated. The active species for the reaction was assigned to be a high valent Ru^{V}=O or Ru^{VI}=O species. The oxo ligand was generated from the ligand-exchange reaction involving the dmso attached to [Ru(babp)(dmso)L]. Some complexes having a labile ligand at an axial position gave a Ru^{VI}=O species as an active intermediate, and others having moderate coordinating one gave a Ru^{V}=O one. The oxidation activities of these complexes were affected by the axial ligand, L, through the *trans*-influence.

Ruthenium(IV, V, or VI)–oxo (Ru=O) species, generated from the reaction of low-valent ruthenium(II or III) complexes and various oxidants, are considered as active intermediates in oxygen-transfer reactions.[1–8] In order to characterize the oxo species generated upon ruthenium complex, mechanistic investigations have been carried out using tripodal polypyridylamine derivatives[9–11] or porphyrin ligands.[12,13] In the case of [Ru^{IV}(bpy)$_2$(py)(O)] complex, the Ru^{IV}=O species had only slight epoxidation activity, while it had good hydrogen atom abstraction activity.[14] Meyer et al. have also reported that the Ru^{IV}=O species attacked the C–H bond rather than olefin double bond and that the low-valent metal–oxo species had radical character.[15] On the other hand, the higher oxidation state of ruthenium–oxo species, such as Ru^{V}=O or Ru^{VI}=O, has epoxidation activity.[2–5] Recently, we have reported that the ruthenium complexes with tripodal tris(2-pyridylmethyl)-amine derivatives catalyzed the hydroxylation of adamantane and epoxidation of cyclohexene in the presence of PhIO, in which the oxidation activity was affected by the electronic and steric character of the ruthenium–oxo species.[16] This complementary reactivity for hydroxylation or epoxidation catalyzed by the Ru=O species is controlled by the substituent group on the pyridylmethylamine ligands. However, this is not sufficient for understanding the characteristics of the Ru=O species, because the bulky pivalamido or neopentylamino groups attached at the 6-position of the pyridine sterically suppress the reactions[16] and the α-position of the pyridine group is often hydroxylated during the reaction.[9,10] In order to avoid self-decomposition of the complex and to have the intermolecular oxygen-transfer reaction occur smoothly, rational design of the coordination structure of the complex is required.

For investigating the characteristics of the Ru=O species, porphyrin has been used as a square-planar ligand.[8,13,17–19] The oxo species on a ruthenium porphyrin complex is located at the axial position of the octahedron. Dissociation of the axial ligand modulated by changes in the field strength of the ligand at the *trans*-position has been discussed using ruthenium nitrosyl complexes with tetradentate planar ligand.[20] The activity of the metal–oxo species at the axial position is regulated by the ligand coordinated at the *trans*-position. Moreover, the catalytic activity in cytochrome P-450 is known to be affected by the axially coordinated proximal ligand to the iron–oxo species.[19–22] Taking into account of the *trans*-influence, the catalytic activity of the metal–oxo species with square-planar ligand has been investigated using non-porphyrin ligand (Scheme 1). In this article, we report the relationship between the coordination structures of the ruthenium complexes with a

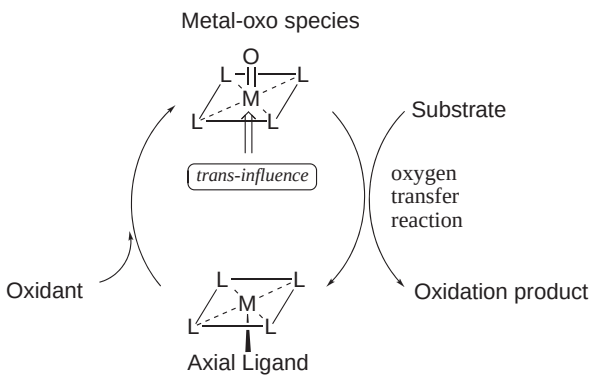

Scheme 1. Oxygen-transfer reaction adjusted by the *trans*-influence of axially coordinating ligand.

Published on the web March 13, 2007; doi:10.1246/bcsj.80.507

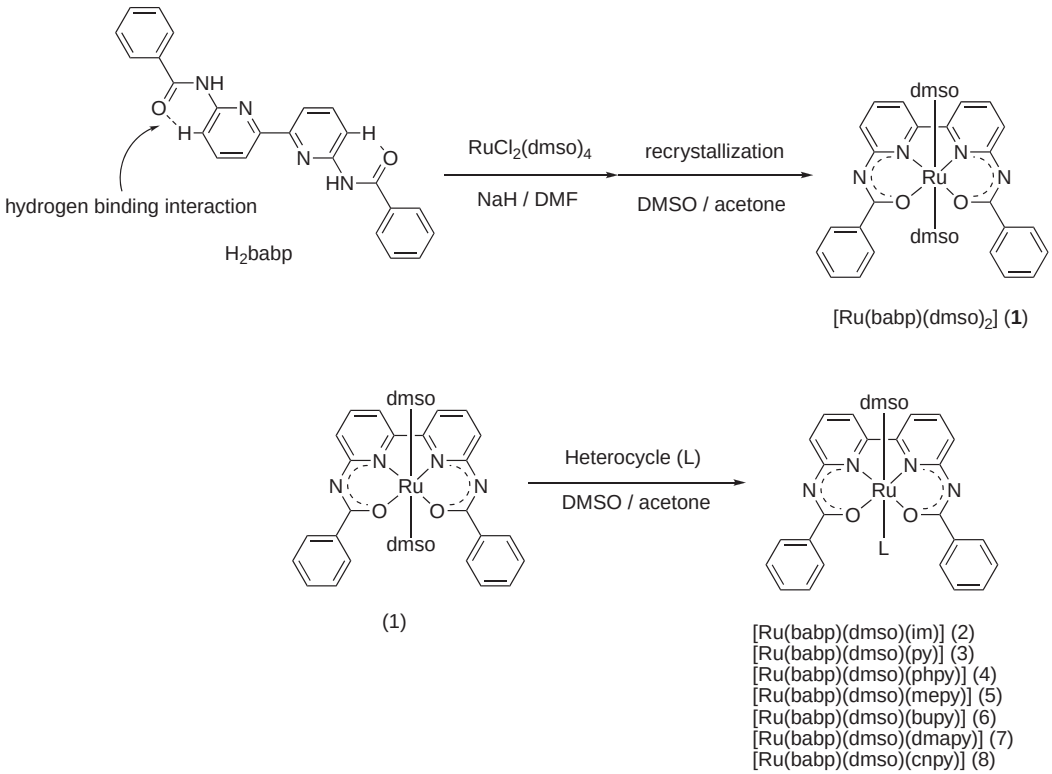

Scheme 2. Intramolecular interaction of BABP and preparation of the ruthenium(II) complexes with babp, [Ru(babp)(dmso)L].

square-planar ligand and their catalytic activities toward oxygen-transfer reactions, which are adjusted by the axial ligand. Ruthenium complexes used here consist of a tetradentate square-planar ligand, 6,6′-bis(benzoylamino)-2,2′-bipyridinato (babp),[23] and two monodentate axial ligands. The babp ligand should not decompose during oxidation,[24–26] which is a key factor for the preparation of a high-performance catalyst. The effect of the axial ligand on the reactivity for the ruthenium-catalyzed oxidation is investigated.

Results and Discussion

Synthesis and Characterization of Ruthenium Complexes. The reaction of *cis*-[$RuCl_2(dmso)_4$] and BABP in the presence of NaH in DMF solution gave [$Ru(babp)(dmso)_2$] complex (**1**). When $RuCl_3$ was used instead of *cis*-[$RuCl_2(dmso)_4$], complex **1** was not obtained. In the positive ion electrospray ionization mass spectrum (ESI-MS) of **1** in methanol solution, peak clusters were observed at $m/z = 495.0$ (100%), 527.0 (17%), 573.2 (7%), corresponding to $[Ru^{II}(babp) + H]^+$, $[Ru^{II}(babp)(CH_3OH) + H]^+$, and $[Ru^{II}(babp)(dmso) + H]^+$, respectively.

Complexes **2**–**8** were synthesized from complex **1** in DMSO solution by the addition of heterocycles, such as imidazole (im), pyridine (py), 4-phenylpyridine (phpy), 4-methylpyridine (mepy), 4-*tert*-butylpyridine (bupy), 4-*N*,*N*-dimethylaminopyridine (dmapy), or 4-cyanopyridine (cnpy), respectively. The synthesis of the ruthenium(II) complexes [Ru(babp)(dmso)(im)] (**2**), [Ru(babp)(dmso)(py)] (**3**), [Ru(babp)(dmso)(phpy)] (**4**), [Ru(babp)(dmso)(mepy)] (**5**), [Ru(babp)(dmso)(bupy)] (**6**), [Ru(babp)(dmso)(dmapy)] (**7**), and [Ru(babp)(dmso)(cnpy)] (**8**), having one heterocycle and one dmso ligand at the axial positions is as shown in Scheme 2. Complexes with heterocycles coordinated at both axial positions were not obtained even with prolonged reaction times or in the presence of excess amount of the ligand. Complexes **1**–**8** were fully characterized by spectroscopic and elemental analyses. Complexes **1** and **5**–**7** were characterized by X-ray diffraction. In less-polar solvents, such as dichloromethane, the color of solution of the ruthenium complexes gradually changed from red to green, but in polar solvents, such as DMSO, this color change did not occur under atmospheric conditions. The solution color did not return to the original even upon addition of dmso. In other words, the coordinated dmso ligand dissociates irreversibly in the less-polar solvent. Accordingly, spectroscopic measurements were carried out in polar solvents in order to determine the structure of the complexes, and investigations on the oxidation activity of the complexes were carried out in less-polar solvents so that catalysis proceeded smoothly. These complexes **1**–**8** were used as catalysts for various oxygen-transfer reactions.

In the IR spectra of **1**–**8**, characteristic C=O stretching bands were observed at about 1550 cm^{-1}, while that of free BABP was observed at 1660 cm^{-1}.[24] This finding indicates that two carbonyl groups of BABP coordinate to the metal center. The ruthenium ion in **1**–**8** was a +II oxidation state because the complexes were ESR silent, so that the ^1H NMR spectra of **1**–**8** in DMSO solution could be acquired. The oxidation state of ruthenium is also verified by X-ray analysis, i.e., no counter ions were found in the crystals of the complexes **1** and **5**–**7**. In the ^1H NMR spectra, summarized in Table 1, the large up-field shifts (about 0.9 ppm) of babp-H5 in **1**–**8** were interpreted as the loss of the hydrogen bonding be-

Table 1. ^{1}H NMR Data of Complexes **1**–**8** and Free BABP[a)]

Complex		babp-H3	babp-H4	babp-H5	babp-phenyl
[Ru(babp)(dmso)$_2$]	**1**	8.19	7.98	7.35	8.40
					7.50
					7.48
[Ru(babp)(dmso)(im)]	**2**	8.10	7.88	7.27	8.38
					7.46
					7.45
[Ru(babp)(dmso)(py)]	**3**	8.26	7.95	7.28	8.39
					7.46
					7.45
[Ru(babp)(dmso)(phpy)]	**4**	8.28	7.97	7.30	8.41
					7.47
					7.45
[Ru(babp)(dmso)(mepy)]	**5**	8.24	7.94	7.26	8.38
					7.46
					7.45
[Ru(babp)(dmso)(bupy)]	**6**	8.24	7.93	7.28	8.39
					7.47
					7.45
[Ru(babp)(dmso)(dmapy)]	**7**	8.18	7.90	7.25	8.38
					7.46
					7.44
[Ru(babp)(dmso)(cnpy)]	**8**	8.31	7.97	7.35	8.38
					7.47
					7.45
BABP		8.24	8.03	8.21	8.08
					7.56
					7.64

a) δ ppm from TMS in dmso-d_6 solution.

tween benzoyl carbonyl oxygen and babp-H5 (8.21 ppm in free ligand and 7.35 ppm in **1**).[27] In **2**, the chemical shift values of the bipyridine moiety of BABP were observed in the highest region of all complexes, because im, which has both σ and π electron-donating abilities, has more electron-donating character than the other nitrogen heterocycles.[28] Complex **7** with dmapy, which is an electron-donating ligand, has the highest chemical shift values among complexes **3**–**8**, which have a pyridine ligand, and complex **8** with cnpy as an electron-withdrawing ligand, shows the lowest values. Based on the NMR results, the nature of the axial ligand affects the electrochemical properties of the complexes.

The electrochemical properties of **1**–**8** were investigated by cyclic voltammetry in acetonitrile solution. Quasi-reversible redox couples (Ru^{II}/Ru^{III}) were observed between 460 and 610 mV (vs SCE). The $E_{1/2}$ value of **2** (460 mV) was lower than that of **1** (521 mV). This negative shift in **2** indicates the stabilization of the higher oxidation state through the coordination of the electron-donating im. The redox potential of **7** is lower than that of **8**, indicating that the electron-donating substituent at 4-posion of pyridine more easily adopts the higher oxidation state similar to im. In Fig. 1, **3** ($E_{1/2}$ = 531 mV vs SCE), **4** (568 mV), **5** (528 mV), **6** (540 mV), **7** (464 mV), and **8** (613 mV), which have pyridine-based ligands, show a good relationship between their redox potentials and the Hammett σ constants for the 4-position of pyridine. In other words, the electronic properties of these ruthenium complexes can be adjusted by the axial ligand.

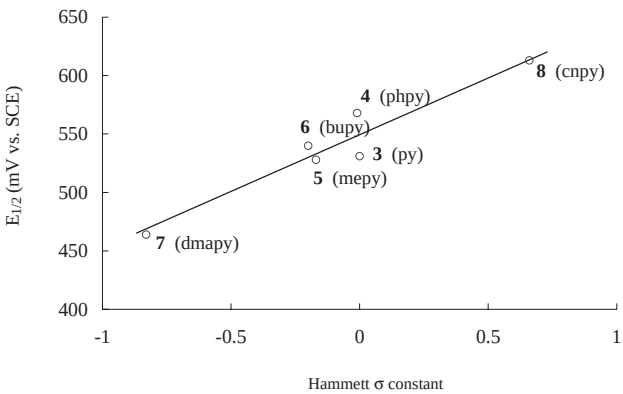

Fig. 1. Relationship between the redox potentials of the complexes (**3**–**8**) and Hammett σ constants of the 4-substituent group of pyridine.

Structural Elucidation of Ruthenium Complexes with Square-Planar Ligand. Complexes **1** and **5**–**7** were obtained as single crystals suitable for X-ray analysis. The crystal data for these complexes except **5**, which has been reported previously,[26] are summarized in Table 2, and selected bond lengths and angles including **5** are listed in Table 3. Complexes **1** and **5**–**7** had an octahedral structure, in which babp coordinated to ruthenium in a square plane and two monodentate ligands, such as dmso or heterocycles, occupied the axial positions (Fig. 2). As expected from their IR spectra, the carbonyl oxygen atoms of the dianionic form of babp[23] were coordinated to

Table 2. Crystallographic Data for Complexes **1**, **6**, and **7**

	[Ru(babp)(dmso)$_2$] **1**[a)]	[Ru(babp)(dmso)(bupy)] **6**	[Ru(babp)(dmso)(dmapy)] **7**
Formula	$(C_{14}H_{14}N_2O_2Ru_{0.5}S)_2$	$C_{36}H_{39}N_5O_4RuS$	$C_{33}H_{34}N_6O_4RuS$
Fw	(324.87) × 2	738.87	711.80
Color	red	red	red
Crystal system	monoclinic	tetragonal	tetragonal
Space group	$C2/c$ (#15)	$I4_1/a$ (#88)	$I4_1/a$ (#88)
a/Å	17.597(1)	20.3664(7)	20.158(1)
b/Å	17.1222(9)		
c/Å	8.8793(5)	32.792(2)	32.238(2)
α/deg			
β/deg	90.590(3)		
γ/deg			
V/Å^3	2675.3(3)	13602.0(9)	13099(1)
Z	8	16	16
ρ_{calcd}/g cm^{-3}	1.613	1.443	1.444
μ/cm^{-1}	7.85	5.69	5.89
F_{000}	1328.00	6112.00	5856.00
R[b)]	0.032	0.071	0.083
Rw[c)]	0.069	0.243	0.248
GOF	0.92	1.48	1.87

a) Complex **1** has a crystallographic two-fold axis passing through the Ru atom and the center of C(1)–C(1′) bond. b) $R = \Sigma||F_0| - |F_c||/\Sigma|F_0|$. c) $Rw = [\Sigma w(F_0^2 - F_c^2)^2/\Sigma w(F_0^2)^2]^{1/2}$; $w = 4F_0^2/\sigma^2(F_0)^2$.

Table 3. Selected Bond Lengths (Å) and Angles (°) of **1**, **5**, **6**, and **7**

	1[a)]	**5**	**6**	**7**
axial ligand	dmso	mepy	bupy	dmapy
Ru–S	2.3055(9)	2.239(3)	2.240(1)	2.240(2)
Ru–N(1c) or Ru–S	2.3055(9)	2.132(8)	2.135(1)	2.158(6)
Ru–O(1a)	2.072(3)	2.082(7)	2.053(4)	2.076(5)
Ru–N(1a)	2.000(3)	1.987(9)	1.984(2)	1.986(6)
Ru–N(1b)	2.000(3)	1.992(9)	1.985(1)	1.992(6)
Ru–O(1b)	2.072(3)	2.071(7)	2.0694(2)	2.063(5)
S–Ru–N(1c) or S–Ru–S	177.64(7)	174.9(2)	177.42(6)	177.5(2)
O(1a)–Ru–N(1a)	93.1(1)	92.8(3)	92.67(9)	91.9(2)
O(1a)–Ru–N(1b)	174.4(1)	173.2(3)	174.48(7)	174.3(2)
N(1a)–Ru–N(1b)	81.5(2)	81.3(4)	82.48(6)	82.7(3)
O(1a)–Ru–O(1b)	92.3(2)	93.9(3)	92.25(8)	92.8(2)

a) Space group was $C2/c$. The molecule **1** has a crystallographic two-fold axis.

the Ru^{II} ion in each complex.

Complex **1** has a crystallographic two-fold axis passing through the Ru atom and the center of C(1)–C(1′) bond. The Ru–S(dmso) bond length was 2.3055(9) Å, which was slightly longer than those observed in $[Ru(NH_3)_5(dmso)]^{2+}$ (2.188(3) Å)[29] and *cis*-$[RuCl_2(dmso)_4]$ (2.252(1)–2.277(1) Å).[30] The longer Ru–S bond lengths, which also occur in the case of *cis*-$[Ru(bpy)_2(dmso)_2]^{2+}$ (2.292(1)–2.293(2) Å), is due to the electron density from back-bonding with the pyridine ligand,[31] and that in the amine complex $[Ru(tpy)(tren)(dmso)]^+$ (2.251(1) Å) is slightly shorter than that of the pyridine complex $[Ru(tpy)(bpy)(dmso)]^+$ (2.282(1) Å).[32] The bond lengths of Ru–S(dmso) in **5**–**7** were slightly shorter than that of **1**, because of the *trans*-influence of the heterocycles. The relatively longer Ru–S(dmso) bond length in the complex **1** indicates a ligand-exchange reaction in the presence of PhIO. In addition, the Ru–N bond lengths of **1** and **5**–**7** (1.984(2)–2.000(3) Å) were slightly shorter than those of Ru–salen (1.997(4)–2.039(5) Å), and the Ru–O bond lengths (2.053(4)–2.082(7) Å) were similar or slightly longer than the salens (2.020(4)–2.063(3) Å).[33]

Oxidation of Olefins and Thioether. The oxidation of *cis*-cyclooctene, *cis*- and *trans*-stilbenes, and thioanisole catalyzed by the typical ruthenium complexes (**1**–**4**) was carried out in the presence of iodosylbenzene (PhIO) as a two-electron oxidant (Ru:substrate:PhIO = 1:100:100) in 1,2-dichloroethane solution at 40 °C for 4 h under argon atmosphere (Scheme 3). These results are summarized in Table 4. Epoxidation of *cis*-cyclooctene catalyzed by **2** gave a 30% yield of 1,2-epoxycyclooctane. Generally, epoxidation of *cis*-cyclooctene catalyzed by ruthenium complexes does not proceed quantitatively. For example, 1,2-epoxycyclooctane is obtained in a 19%

yield when a mononuclear ruthenium(III) complex with Schiff base ligand is used as a catalyst,[34] and Ru^{III}–salen complexes give the epoxide in poor yield in comparison with the corresponding Mn^{III} complexes.[6] In this case, PhIO is known to be an efficient 2-electron oxidant for the generation of Ru=O species,[1,2,5,6,35,36] but has relatively lower epoxidation activity compared with periodate oxidant (IO_4^-).[37] When **4** was used as a catalyst in the place of **2**, only a 4.2% yield of 1,2-epoxycyclooctane was obtained under the same reaction conditions. The order of the yield of 1,2-epoxycyclooctane was **2** > **1** > **3** > **4**, which was identical with the case of oxidation of stilbenes and cyclohexene. When ^{t}BuOOH was used as an oxidant in the presence of **1**, the yield of the corresponding epoxide was 26%. The reactivity of alkylhydroperoxide is similar to that of PhIO. *m*-Chloroperbenzoic acid (MCPBA), which is often used to generate metal–oxo species, was not utilized in our oxidation experiments to avoid further complicated reactions.[3,5,12,13,17,38,39] For our investigations to determine the relationship between the structure and the catalytic activities of the ruthenium complexes, PhIO was used because of ease of handling.[41] In the oxidation of cyclooctene, moreover, no *cis*-cyclooctane-1,2-diol was detected, which means that *cis*-dioxoruthenium(VI) intermediate was not involved in the reaction.[40]

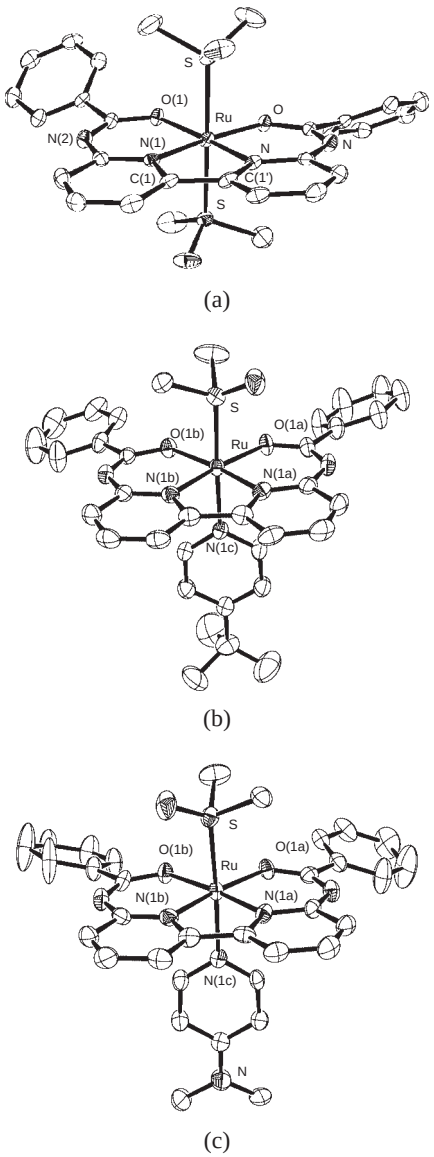

Fig. 2. (a) X-ray structure of **1**. (b) X-ray structure of **6**. (c) X-ray structure of **7**.

Oxidation of *cis*-stilbene catalyzed by **1**–**4** gave *cis*-stilbene oxide, a small amount of *trans*-epoxide, and large amount of benzaldehyde, which was a C=C bond cleavage product. Formation of a thermally stable *trans*-stilbene oxide in the oxidation of *cis*-stilbene suggests a radical intermediate.[2,13,42] In acetonitrile, the epoxidation activity of **1** decreased compared to that in 1,2-dichloroethane, and the ratio for *cis*-stilbene oxide to *trans*-one decreased.[16] Radical pathway is accelerated in halogeno-hydrocarbon.[42,43] In the case of **3** or **4** with pyridine derivative, a significant decrease in the yield of stilbene oxide and increase in that of benzaldehyde were observed. This find-

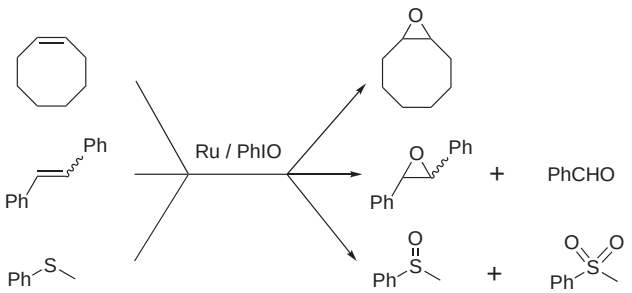

Scheme 3. Oxidation of substrates.

Table 4. Oxidation of Olefins and Thioether Catalyzed by **1**–**4**[a)]

		Cyclooctene	*cis*-Stilbene[b)]			*trans*-Stilbene[b)]			Thioanisole	
[Ru(babp)(dmso)L]		Epoxide /%	*cis*-Epoxide /%	*trans*-Epoxide /%	Benzaldehyde /%	*cis*-Epoxide /%	*trans*-Epoxide /%	Benzaldehyde /%	Sulfoxide[c)] /%	Sulfone[d)] /%
	axial ligand (L)									
1	dmso	24 26[e)]	20	2.2	48	nd[g)]	19	34	41	5.1
			8.2[f)]	1.8[f)]	40[f)]					
2	im	30	28	2.3	32	nd	28	28	23	9.6
3	py	13	7.8	1.3	50	nd	14	44	37	6.8
4	phpy	4.2	6.6	1.4	53	nd	12	45	22	10

a) Reaction conditions: Ru–babp complex:substrate:PhIO = 1:100:100 in 1,2-dichloroethane, 40 °C, 4 h, under Ar. b) Ref. 26. c) Methylphenylsulfoxide. d) Methylphenylsulfone. e) ^{t}BuOOH was used as an oxidant instead of PhIO. f) Acetonitrile was used as a solvent instead of 1,2-dichroloethane. g) nd = not detected.

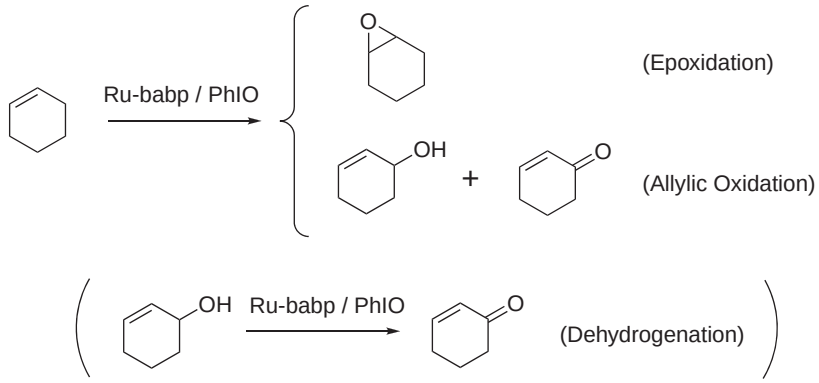

Scheme 4.

ing is similar to a previous report that the epoxidation of *trans*-stilbene catalyzed by the combined system of $RuCl_3$, $NaIO_4$, and chiral bis(dihydrooxazolylphenyl)oxalamide ligand gave a moderate yield (4–43%) of the corresponding epoxide accompanied by significant amount (21–65% yield) of benzaldehyde.[44] In the oxidation of stilbenes catalyzed by the high-valent ruthenium–oxo species with a non-porphyrin ligand, C=C bond cleavage reactions predominantly have been reported to occur.[4] Using ruthenium–porphyrin complex, however, selectivity for the cleavage reaction is quite low.[45] This finding indicates that babp acts as a non-porphyrin ligand, even though it adopts square-planar 4-coordination geometry with the expanded resonant system. In the oxidation of *trans*-stilbene, **1**–**4** had similar reactivity to that with *cis*-stilbene, although *cis*-stilbene oxide was not detected. In these reactions, formation of benzaldehyde relatively decreased in comparison with the cases of *cis*-one.

Oxidation of thioanisole catalyzed by **1**–**4** gave methylphenylsulfoxide and methylphenylsulfone. The sulfone is successive oxidation product of the sulfoxide. In the oxidation of thioether, an electrophilic oxygen species gave a sulfoxide, but a nucleophilic one did not show any reactivity.[46] On the other hand, sulfone is generated from the corresponding sulfoxide using either an electrophilic or nucleophilic active oxygen species.[47] Formation of methylphenylsulfoxide and methylphenylsulfone in this system indicates that the active species derived from **1**–**4** has electrophilic and nucleophilic characters.

Effect of Axial Ligands. Oxidation of cyclohexene catalyzed by **1**–**8** was carried out at 40 °C for 4 h under argon in the presence of PhIO (Ru:olefin:PhIO = 1:100:100) in 1,2-dichloroethane. This reaction gave 1,2-epoxycyclohexane as an epoxidation product and both 2-cyclohexen-1-ol and 2-cyclohexen-1-one as allylic oxidation products as shown in Scheme 4. In this ruthenium–PhIO system, alcohol was easily oxidized to ketone.[48] It is well known that cyclohexene is sensitive toward allylic oxidation,[49] but *cis*-cyclooctene hardly takes place allylic oxidation.[50] Using iron(III)– or manganese(III)–porphyrin and PhIO system, influence of the ring size of the cycloalkenes on the selectivity for epoxidation and allylic oxidation has been studied.[51] Epoxidation activity of **2** was superior to those of the other complexes as summarized in Table 5. The yields of 1,2-epoxycyclohexane decreased in the order of **2** > **1** > **3** > **4**, which was similar to the case of *cis*-cyclooctene as mentioned above. All ruthenium complexes except **7** showed moderate reactivity for epoxidation at 40 °C. The epoxidation activity of **2** increased at 80 °C. In the reaction catalyzed by **7**, the yield of the oxidation products was very low at 40 °C. The yield of 1,2-epoxycyclooctane was 0.8%. At 80 °C, however, **7** showed higher catalytic activity, and the yield of 1,2-epoxycyclohexane rose to 51% accompanied by 20% of the allylic oxidation products. At 80 °C, the reactivity of **7** is comparable to that of **2**. The dmapy ligand coordinated at the *trans*-position might suppress the ligand-exchange reaction from dmso to oxo species. At higher temperature, however, dissociation of dmso from **7** gave an active species leading to the same reactivity as demonstrated in **2**. In complexes **3**–**6**, their oxidation activities are similar to each other, of which redox potentials are within a range of 40 mV as shown in Fig. 1. From these findings, we believe that the active species generated from the complexes **2**–**7** is common in the catalysis. In the case of **8**, we may consider that the reactivity was the lowest of all complexes here employed because of the coordination of the electron-withdrawing cnpy ligand at the *trans*-position. However, the oxidation activity of **8** was comparable to that of **1** as listed in Table 5. This finding is interpreted in terms of the easy dissociation of cnpy from ruthenium, which is discussed later.

Table 5. Oxidation of Cyclohexene Catalyzed by **1**–**8**[a)]

Complex [Ru(babp)(dmso)L] L		Epoxidation Yield (E) /%	Allylic oxidation Yield (A)[c)] /%	E/A
dmso[b)]	**1**	19	5.6	3.3
im[b)]	**2**	22	6.1	3.7
		54[d)]	12[d)]	4.7[d)]
py[b)]	**3**	10	7.3	1.4
phpy[b)]	**4**	7.5	8.6	0.9
mepy	**5**	11	5.4	2.0
bupy	**6**	10	5.3	1.9
dmapy	**7**	1.8	3.6	0.5
		51[d)]	20[d)]	2.6[d)]
cnpy	**8**	19	7.1	2.6

a) Reaction conditions were the same as those in Table 4. b) Ref. 26. c) Total yields of 2-cyclohexen-1-ol and 2-cyclohexen-1-one. d) 80 °C, 2 h.

The ratio (E/A) of epoxidation to allylic oxidation describes an interesting catalytic activity of the ruthenium complexes.

Here, the allylic oxidation products include both 2-cyclohexen-1-ol and 2-cyclohexen-1-one, because the allylic alcohol once formed is further oxidized to give an α,β-unsaturated ketone through the ruthenium-catalyzed oxidative dehydrogenation pathway.[16,36,48] In the reactions catalyzed by **1**–**8**, E/A in Table 5 was in range of about 0.5–3.7, which was almost constant during the initial stage of the reaction. Using tripodal pyridylmethylamine ligands, the ratios 21 using $[Ru^{II}(bppa)Cl]PF_6$ and 6.3 using $[Ru^{III}(bnpa)Cl_2]PF_6$ have been reported.[16] Such a difference in the reactivity has been interpreted in terms of the *trans*-influence of tertiary amine or pyridine of the tripodal ligands. We think that the oxo-species generated with bppa complex is an electrophilic Ru^{V}=O species and that with bnpa complex is a radical Ru^{IV}–O• species. The catalytic intermediate in these reactions is thought to be combination of both Ru^{V}=O and Ru^{IV}–O•, which are electronically equivalent to each other.[52] The amine- or pyridine-nitrogen atom that occupies *trans*-position of the oxo species affects the intermediate.[52,53] In the reactions catalyzed by **1**–**8**, the axial ligand coordinated at *trans*-position to the ruthenium–oxo species obviously causes *trans*-influence for the reactivity. The ratio in **2** was higher than those in **3**–**6**. When the electron-donating im was used as an axial ligand, the epoxidation activity for cyclohexene was relatively high, but the allylic oxidation activity was low. On the other hand, such selectivity was not observed when pyridine derivatives were used. The effect of donor ligand has also been reported in the case of Cr(salen)- or Mn(salen)-catalyzed epoxidation of olefins.[53]

Spectroscopic Characterization of Ruthenium–Oxo Species. Characterization of the transient species generated from the starting ruthenium complex and PhIO was carried out using the UV–vis and ESI-MS spectroscopic methods. The color change of the reaction solution from reddish-yellow of the starting ruthenium(II) species to reddish-purple after addition of PhIO indicates a transient ruthenium species. In the reaction of **1** and PhIO, typical absorption bands in UV–vis spectrum were observed at 377 and 394 nm ($\varepsilon = 5700$ and 6400 $M^{-1}\,cm^{-1}$, respectively). They are assigned to spin-allowed $p\pi(O^{2-}) \rightarrow Ru^{VI}$ charge-transfer (CT) band, because the characteristic absorption bands of Ru=O species with nitrogen-containing ligands are generally observed at about 380–400 nm.[39,54] This CT band disappeared after addition of cyclohexene. Spectral changes in the reaction solution of **1** with successive addition of PhIO and cyclohexene in 1,2-dichloroethane are shown in Fig. 3. Moreover, the ESR signal of the solution containing **1** and PhIO was silent. These findings indicate that the oxidation state of the starting ruthenium **1** is +II and that of active species generated by the reaction with PhIO is +IV or +VI. On the other hand, such color change as observed with **1** did not occur with **2**–**4**. The Ru=O species generated from **2**–**4** and PhIO is different from that from **1**. Detailed characterization of the active species from **2**–**4** was impossible using NMR spectroscopy because of their paramagnetic characters. Accordingly, we think that the oxidation state of the active species generated from **2**–**4** is +V.

ESI-MS is known to be a useful tool for characterization of large size biomolecules and multiply charged metal complexes in solution because of its mild ionization method.[55] Detection of prominent peak clusters of $[O{=}Mn^{V}(salen)]^+$ complex, as a metastable transient species, in a mixture of $[Mn^{III}(salen)]^+$ and PhIO has been reported.[56] In positive mode ESI-MS in a 1/10 (v/v) 1,2-dichloroethane/acetonitrile solution, several spectral patterns were observed in the reaction mixture of the [Ru(babp)(dmso)L] and PhIO. In the case of **1**, peak clusters were observed at $m/z = 527.1$ (100%), 510.1 (20%), and 494.1 (35%), corresponding to the $[Ru^{VI}(babp)(O)_2 + H]^+$, $[Ru^{IV}(babp)(O) + H]^+$, $[Ru^{III}(babp)]^+$ ions, respectively, although unidentified higher molecular peak clusters were detected at $m/z = 563.2$ and 552.1. The isotopic patterns of Ru^{VI} species at $m/z = 527.1$ agreed with those calculated for $[Ru^{VI}(babp)(O)_2 + H]^+$ or $[Ru^{VI}(babp)(O)(OH)]^+$, as shown in Fig. 4. Although we have no information whether formula of $[Ru^{VI}(babp)(O)_2 + H]^+$ or $[Ru^{VI}(babp)(O)(OH)]^+$ is correct, formation of Ru^{VI}=O species as expected from the UV–vis and ESR spectra is confirmed by ESI-MS. In the presence of PhIO, the starting complex **1** easily released two dmso ligands from ruthenium to give oxo species accompanied with oxidation of Ru^{II} to Ru^{VI}. In the case of **2**, a peak cluster was observed at $m/z = 578.3$ (100%) corresponding to $[Ru^{V}(babp)(im)(O)]^+$ ions, as shown in Fig. 5. Substitutionally labile dmso in **2** was exchanged with an oxo ligand, and substitutionally inert im remained in the transient species. Some of the differences observed in the reactivity of **1** and **2** are interpreted in terms of the oxidation state of the transient ruthenium species.

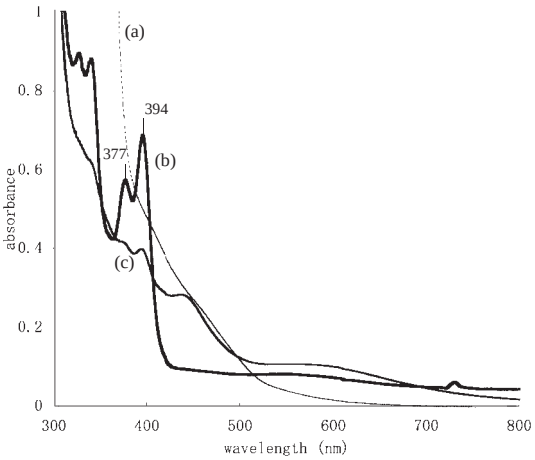

Fig. 3. Spectral change of **1** in 1,2-dichloroethane solution with successive addition of PhIO and cyclohexene. (a) Starting solution of **1** (0.1 mM). (b) Addition of PhIO (100 equiv) to (a). (c) Successive addition of cyclohexene (100 equiv) to (b).

The ESI-MS of the reaction of **7** and PhIO had a peak cluster at $m/z = 693.9$ (100%), corresponding to $[Ru^{III}(babp)(dmapy)(dmso)]^+$ ions. No Ru=O species thought to be the active oxygen species were detected in the same analysis condition in **1** and **2**. It is concluded that the poor catalytic activity of **7** at 40 °C is because no active species forms. Complex **7** having electron-donating dimethylamino group was expected to have similar activity to that of **2** because of their $E_{1/2}$ values, but it had almost no reactivity at 40 °C. At higher temperature, **7** became reactive, because dmso dissociated to afford the active species in the presence of PhIO. Complex **8**, which has an electron-withdrawing cyano group, was expected to

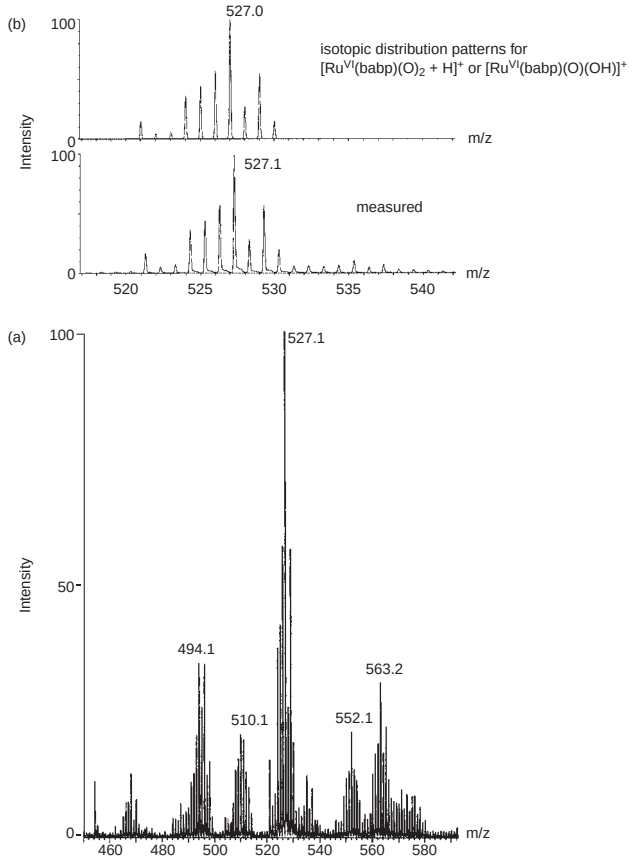

Fig. 4. Positive mode ESI-MS of the reaction mixture of **1** and PhIO. (a) Mass spectral pattern within the range $m/z = 460$–580. (b) Peak clusters assigned to Ru^{VI}=O species.

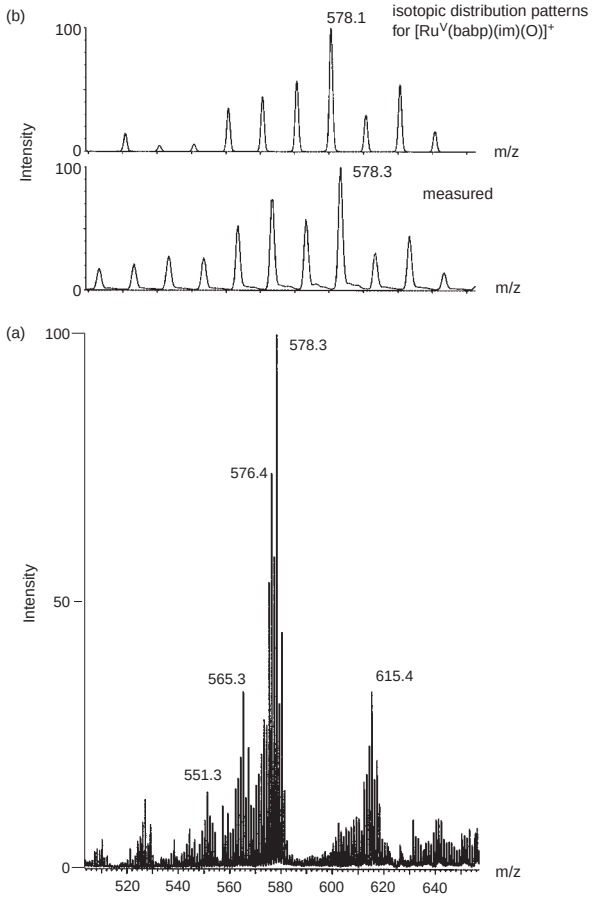

Fig. 5. Positive mode ESI-MS of the reaction mixture of **2** and PhIO. (a) Mass spectral pattern within the range $m/z = 520$–640. (b) Peak clusters assigned to Ru^{V}=O species.

have the lowest reactivity, because it has the most positive $E_{1/2}$ value of all complexes. In the reaction catalyzed by **8**, however, the oxidation activity as listed in Table 5 was similar to that of **1**. The changes in the spectra of the reaction solution containing **8** upon successive additions of PhIO and cyclohexene were similar to those of **1**. ESI-MS spectrum of the mixture of **8** and PhIO also had peak clusters at $m/z = 638.9$ (8%) and 676.9 (100%). The former was assigned to $[Ru^{VI}(babp)(O)_2(C_2H_6SO_2)(H_2O)]^+$ ion, with which isotopic pattern fully agreed, but the formation pathway is not clear yet. The latter was assigned to $[Ru^{III}(babp)(cnpy)(dmso)]^+$. Formation of Ru^{VI}=O from **8** was confirmed by ESI-MS, even though the starting complex remained. The weakly coordinated axial ligand, cnpy, dissociates from **8** to generate the Ru^{VI}=O species.

Conclusion

Eight ruthenium(II) complexes, [Ru(babp)(dmso)L], consisting of the tetradentate babp and two monodentate ligands, DMSO and L (L = DMSO or heterocycles), were prepared. All complexes had an octahedral geometry with square-planar coordination of babp. Complexes **1**–**8** showed moderate catalytic activities toward the oxygen-transfer reactions, such as epoxidation, allylic oxidation, and bond cleavage of olefins and sulfoxidation of thioethers, in the presence of PhIO. The catalytic activity of the high-valent ruthenium–oxo species, generated from the ligand-exchange reaction of dmso and oxidant, was affected by the *trans*-influence of the axial ligand. The order of epoxidation activity of [Ru(babp)(dmso)L] complexes (**1**–**8**) was as follows: **2** (L = im) > **1** (L = dmso) > **3**–**8** (L = pyridine derivatives). Weakly coordinated ligands, such as dmso or cnpy, are easily exchanged to afford the oxo species Ru^{VI}=O in the presence of PhIO. Strongly coordinated dmapy prevents ligand-exchange reaction at low temperature. Moderately coordinated ligand, such as im or pyridine derivatives, gives Ru^{V}=O intermediate. The catalytic activities of mononuclear ruthenium–oxo complexes with the square-planar ligand are controlled by axial ligand coordinating at the *trans*-position. Rational design of the coordination structure of the catalyst precursor, leading to the active species, is important for selective oxygen-transfer reactions.

Experimental

Materials and Measurement. Reagents used for synthesis were of the highest grade available and were used without further purification. All solvents for spectroscopic measurements, except NMR spectroscopy, were purified by distillation before use. BABP was prepared according to the method previously reported.[24]

UV–vis spectra were recorded on a JASCO Ubest-570. ^{1}H NMR spectra were measured on a Varian VXR-300S spectrometer with TMS as an internal standard. The redox potentials ($Ru^{II/III}$) of

the complexes were measured in CH_3CN solution using a BAS CV-1 cyclic voltammetry unit. All measurements were carried out at room temperature with a sweep rate of 50 or 100 V s^{-1} under Ar using $^nBu_4NPF_6$ as a supporting electrolyte and referenced to SCE. ESR spectra were measured with a JEOL JES-REIX spectrometer at 77 K. IR spectra measured for a KBr pellet were performed on a JASCO FT/IR-410. GC analysis using an internal standard method was performed on a Shimadzu GC8F apparatus equipped with PEG-20M or silicon OV-17 column. Positive mode of ESI-MS spectra for characterization of Ru=O species generated from the mixture of ruthenium complex and 10 equiv of PhIO in 1,2-dichloromethane solution were aquired on a Micromass LCT, to which 10-fold amount of acetonitrile was added for easy ionization. The isotopic patterns of the complexes agree with those calculated for the given formulations.

Crystal Structure Analysis. Single crystals of **1** and **5–7** suitable for X-ray diffraction measurements were mounted on a glass capillary, and the diffraction data were collected for **1**, **6**, and **7** on a Rigaku MSC Mercury CCD using graphite monochromated Mo Kα radiation ($\lambda = 0.71070$ Å) and for **5** on a Rigaku RAXIS-II imaging plate area detector using graphite monochromated Mo Kα radiation. All of the structures were solved by a combination of direct method and Fourier techniques. Non-hydrogen atoms were anisotropically refined by full-matrix least-squares calculations. Hydrogen atoms were included but not refined. Refinements were continued until all shifts were smaller than one-third of the standard deviations of the parameters involved. R and Rw values were defined as follows:[57] $R = \Sigma||F_0| - |F_c||/\Sigma|F_0|$ and $Rw = [\Sigma w(F_0^2 - F_c^2)^2/\Sigma w(F_0^2)^2]^{1/2}$, $w = 4F_0^2/\sigma^2(F_0)^2$. Atomic scattering factors and anomalous dispersion terms were taken from International Tables for X-ray Crystallography.[58] All calculations were carried out on a Japan SGI workstation computer using the teXsan crystallographic software package.[59] Crystallographic data has been deposited with Cambridge Crystallographic Data Centre: Deposition number CCDC-622758 for compound **1**, -622759 for **6**, and -622760 for **7**. Copies of the data can be obtained free charge via http://www.ccdc.cam.ac.uk/conts/retrieving.html (or from the Cambridge Crystallographic Data Centre, 12, Union Road, Cambridge, CB2 1EZ, UK; Fax: +44 1223 336033; e-mail: deposite@ccdc.cam.ac.uk).

Synthesis and Characterization of the Ruthenium Complexes. [Ru^{II}(babp)(dmso)$_2$] (1): To a solution of BABP (0.26 g, 0.65 mmol) in DMF (80 mL) was added excess amount of NaH (0.07 g) and equimolar amount of *cis*-[$RuCl_2$(dmso)$_4$] (0.32 g). The mixture was refluxed for 3 h under nitrogen atmosphere. After evaporation of the solvent, small amounts of DMSO and acetone were added to the residue. An orange crystal (0.23 g, 55% yield) of [Ru^{II}(babp)(dmso)$_2$] complex (**1**) suitable for X-ray analysis precipitated from the solution.

IR (KBr, cm^{-1}): 1552 (C=O). Anal. Calcd for **1** ($C_{28}H_{28}N_4O_4S_2Ru\cdot 0.1H_2O$): C, 51.62; H, 4.36; N, 8.60%. Found: C, 51.41; H, 4.47; N, 8.84%. Positive mode ESI-MS (methanol): m/z = 495.0 (100%), 527.0 (17%), 573.2 (7%), corresponding to [Ru^{II}(babp) + H]$^+$, [Ru^{II}(babp)(CH_3OH) + H]$^+$, and [Ru^{II}(babp)(dmso) + H]$^+$ ions, respectively. ^{1}H NMR data are summarized in Table 1, in which the chemical shift values of the coordinating $(CH_3)_2SO$ moiety of all complexes are not characterized because of scrambling of the ligand (dmso-h_6) and the solvent (dmso-d_6). Complex **1** has a crystallographic two-fold axis passing through the Ru atom and the center of C(1)–C(1′) bond, so the environments of the above and below structures of the complex are the same each other. Crystallographic data are listed in Table 2, and selected bond lengths and angles are listed in Table 3.

[Ru(babp)(dmso)(im)](2): To complex **1** (37 mg, 0.057 mmol) under nitrogen atmosphere was added a DMSO solution (3 mL) of im (39 mg, 0.57 mmol). The mixture was stirred for 3 days at room temperature. The cloudy reaction solution became clear dark red, to which acetone was added. On standing, a small amount of precipitate was obtained. In the preparation of **2–8**, isolated yields of the ruthenium(II) complexes precipitated from the reaction solution were about 50% based on the starting **1**.

IR (KBr, cm^{-1}): 1550 (C=O). Anal. Calcd for **2** ($C_{29}H_{26}N_6O_3SRu\cdot 0.5H_2O$): C, 53.69; H, 4.20; N, 12.96%. Found: C, 53.66; H, 4.09; N, 12.74%. ^{1}H NMR data for **2** are summarized in Table 1.

[Ru(babp)(dmso)L] (3–8): Complexes **3–8** with pyridine derivatives were synthesized similar to **2**. ^{1}H NMR data are summarized in Table 1.

[Ru(babp)(dmso)(py)] (**3**): Red crystal. IR (KBr, cm^{-1}): 1550 (C=O). Anal. Calcd for **3** ($C_{31}H_{27}N_5O_3SRu\cdot 0.2DMSO$): C, 56.60; H, 4.27; N, 10.51%. Found: C, 56.84; H, 4.23; N, 10.24%.

[Ru(babp)(dmso)(phpy)] (**4**): Dark red crystal. IR (KBr, cm^{-1}): 1548 (C=O). Anal. Calcd for **4** ($C_{37}H_{31}N_5O_3SRu\cdot 0.4H_2O$): C, 60.54; H, 4.37; N, 9.54%. Found: C, 60.28; H, 4.23; N, 9.25%.

[Ru(babp)(dmso)(mepy)] (**5**): Orange crystal. IR (KBr, cm^{-1}): 1549 (C=O). Anal. Calcd for **5** ($C_{32}H_{29}N_5O_3SRu\cdot 0.5$acetone): C, 58.00; H, 4.65; N, 10.09%. Found: C, 57.84; H, 4.45; N, 9.99%. The crystal structure of **5** obtained from recrystallization in acetone solution was reported previously.[26] Selected bond lengths and angles are listed in Table 3.

[Ru(babp)(dmso)(bupy)] (**6**): Orange crystal. IR (KBr, cm^{-1}): 1551 (C=O). Anal. Calcd for **6** ($C_{35}H_{35}N_5O_3SRu\cdot$DMSO): C, 56.61; H, 5.62; N, 8.92%. Found: C, 56.90; H, 5.43; N, 8.87%. Crystallographic data are listed in Table 2, and selected bond lengths and angles are listed in Table 3.

[Ru(babp)(dmso)(dmapy)] (**7**): Orange crystal. IR (KBr, cm^{-1}): 1548 (C=O). Anal. Calcd for **7** ($C_{33}H_{32}N_6O_3SRu\cdot$DMSO): C, 54.46; H, 4.96; N, 10.89%. Found: C, 54.67; H, 5.07; N, 11.04%. Crystallographic data are listed in Table 2, and selected bond lengths and angles are listed in Table 3.

[Ru(babp)(dmso)(cnpy)] (**8**): Orange Crystal. IR (KBr, cm^{-1}): 1551 (C=O). Anal. Calcd for **8** ($C_{32}H_{26}N_6O_3SRu\cdot H_2O$): C, 55.40; H, 4.07; N, 12.11%. Found: C, 55.33; H, 4.00; N, 12.00%.

Oxidation of Substrates. Oxidation of substrate (cyclooctene 55 mg, *cis*- and *trans*-stilbenes 90 mg, cyclohexene 41 mg, or thioanisole 62 mg (0.5 mmol)) was carried out in the presence of PhIO (110 mg, 0.5 mmol) and the ruthenium complex (0.005 mmol) in 1,2-dichloroethane (5 mL) under Ar atmosphere at 40 °C. The reaction products identified by comparison with the authentic samples were monitored by GC analysis at appropriate time.

Measurement of Spectral Change of the Complex 1. UV–vis spectra of the complex **1** was measured in the 1,2-dichloroethane solution (0.1 mM) at room temperature, to which 100-fold amount of PhIO was added and stirred at room temperature under Ar atmosphere. Absorption maxima as CT bands were observed at 377 and 394 nm. ESI-MS was measured under these conditions with addition of acetonitrile. To examine the reactivity of this reaction solution, 100-fold amount of cyclohexene was added. The CT bands were disappeared after addition of cyclohexene. These results are shown in Fig. 3.

This work was supported by a Grant-in-Aid for Scientific Research from the Ministry of Education, Culture, Sports, Science and Technology Japan, to which our thanks are due.

References

1 D. Ostovic, T. C. Bruice, *Acc. Chem. Res.* **1992**, *25*, 314.

2 B. Meunier, *Chem. Rev.* **1992**, *92*, 1411.

3 a) C.-M. Che, V. W.-W. Yam, *Adv. Inorg. Chem.* **1992**, *39*, 233. b) T. Naota, H. Takaya, S.-I. Murahashi, *Chem. Rev.* **1998**, *98*, 2599.

4 W. P. Griffith, *Chem. Soc. Rev.* **1992**, *21*, 179.

5 G. A. Braf, R. A. Sheldon, *J. Mol. Catal. A: Chem.* **1995**, *102*, 23.

6 K. Nakata, T. Takeda, J. Mihara, R. Irie, T. Katsuki, *Chem. Eur. J.* **2001**, *7*, 3776.

7 M. H. V. Huynh, L. M. Witham, J. M. Lasker, M. Wetzier, B. Mort, D. L. Jameson, P. S. White, K. J. Takeuchi, *J. Am. Chem. Soc.* **2003**, *125*, 308.

8 J.-L. Zhang, C.-M. Che, *Chem. Eur. J.* **2005**, *11*, 3899.

9 a) C.-M. Che, V. W.-W. Yam, T. C. W. Mak, *J. Am. Chem. Soc.* **1990**, *112*, 2284. b) T. Kojima, *Chem. Lett.* **1996**, 121. c) M. Yamaguchi, H. Kousaka, T. Yamagishi, *Chem. Lett.* **1997**, 769.

10 T. Kojima, H. Matsuo, Y. Matsuda, *Inorg. Chim. Acta* **2000**, *300–302*, 661.

11 T. Kojima, K. Hayashi, Y. Matsuda, *Inorg. Chem.* **2004**, *43*, 6793.

12 W.-H. Fung, W.-Y. Yu, C.-M. Che, *J. Org. Chem.* **1998**, *63*, 7715.

13 C.-J. Liu, W.-Y. Yu, C.-M. Che, C.-H. Yeung, *J. Org. Chem.* **1999**, *64*, 7365.

14 J. M. Bryant, T. Matsuo, J. M. Mayer, *Inorg. Chem.* **2004**, *43*, 1587.

15 L. K. Stultz, M. H. V. Huynh, R. A. Binstead, M. Curry, T. J. Meyer, *J. Am. Chem. Soc.* **2000**, *122*, 5984.

16 a) K. Jitsukawa, Y. Oka, H. Einaga, H. Masuda, *Tetrahedron Lett.* **2001**, *42*, 3467. b) K. Jitsukawa, Y. Oka, S. Yamaguchi, H. Masuda, *Inorg. Chem.* **2004**, *43*, 8119.

17 T.-S. Lai, H.-L. Kwong, R. Zhang, C.-M. Che, *J. Chem. Soc., Dalton Trans.* **1998**, 3559.

18 J.-S. Huang, X.-R. Sun, S. K.-Y. Leung, K.-K. Cheung, C.-M. Che, *Chem. Eur. J.* **2000**, *6*, 334.

19 K. Auclair, P. Moenne-Loccoz, P. R. Ortiz de Montellano, *J. Am. Chem. Soc.* **2001**, *123*, 4877, and references cited therein.

20 A. K. Patra, M. J. Rose, K. A. Murphy, M. M. Olmstead, P. K. Mascharak, *Inorg. Chem.* **2004**, *43*, 4487.

21 *Cytochrome P-450: Structure, Mechanism and Biochemistry*, 2nd ed., ed. by P. R. Ortiz de Montellano, Plenum Press, New York, **1995**.

22 P. K. Sharma, S. P. de Visser, F. Ogliaro, S. Shalik, *J. Am. Chem. Soc.* **2003**, *125*, 2291.

23 6,6′-Bis(benzoylamino)-2,2′-bipyridine, BABP = H_2babp. Deprotonated coordination form in the complexes is expressed babp.

24 M. Yamada, K. Araki, S. Shiraishi, *Bull. Chem. Soc. Jpn.* **1987**, *60*, 3149.

25 K. Araki, T. Kuboki, M. Otohata, N. Kishimoto, M. Yamada, S. Shiraishi, *J. Chem. Soc., Dalton Trans.* **1993**, 3647.

26 K. Jitsukawa, H. Shiozaki, H. Masuda, *Tetrahedron Lett.* **2002**, *43*, 1491.

27 S. Yamaguchi, A. Kumagai, S. Nagatomo, T. Kitagawa, Y. Funahashi, T. Ozawa, K. Jitsukawa, H. Masuda, *Bull. Chem. Soc. Jpn.* **2005**, *78*, 116.

28 a) C. R. Johnson, C. M. Jones, S. A. Asher, J. E. Abola, *Inorg. Chem.* **1991**, *30*, 2120. b) S. Asperger, B. Cetina-Cizmek, *Inorg. Chem.* **1996**, *35*, 5232.

29 F. C. March, G. Ferguson, *Can. J. Chem.* **1971**, *49*, 3590.

30 A. Mercer, J. Trotter, *J. Chem. Soc., Dalton Trans.* **1975**, 2480.

31 M. K. Smith, J. A. Gibson, C. G. Young, J. A. Broomhead, P. C. Junk, F. R. Keene, *Eur. J. Inorg. Chem.* **2000**, 1365.

32 A. A. Rachford, J. L. Petersen, J. J. Rack, *Inorg. Chem.* **2005**, *44*, 8065.

33 a) W. Odenkirk, A. L. Rheingold, B. Bosnich, *J. Am. Chem. Soc.* **1992**, *114*, 6392. b) K. Omura, T. Uchida, R. Irie, T. Katsuki, *Chem. Commun.* **2004**, 2060.

34 M. J. Upadhyay, P. K. Bhattacharya, P. A. Ganesphure, S. Satish, *J. Mol. Catal.* **1992**, *73*, 277.

35 a) P. Müller, J. Godoy, *Tetrahedron Lett.* **1981**, *22*, 2361. b) M. Bressan, A. Morvillo, *Inorg. Chem.* **1989**, *28*, 950. c) C.-M. Che, *Pure Appl. Chem.* **1995**, *67*, 225.

36 A. Morvillo, M. Bressan, *J. Mol. Catal. A: Chem.* **1997**, *125*, 119.

37 A. J. Bailey, W. P. Griffith, P. D. Savage, *J. Chem. Soc., Dalton Trans.* **1995**, 3537.

38 a) C.-M. Che, C. Ho, T.-C. Lau, *J. Chem. Soc., Dalton Trans.* **1991**, 1259. b) Z. Gross, S. Ini, *J. Org. Chem.* **1997**, *62*, 5514. c) V. C. Catalano, R. A. Heck, C. E. Immoos, A. Ohaman, M. G. Hill, *Inorg. Chem.* **1998**, *37*, 2150. d) M. Renz, B. Meunier, *Eur. J. Org. Chem.* **1999**, 737.

39 L. K. Stultz, R. A. Binstead, M. S. Reynolds, T. J. Meyer, *J. Am. Chem. Soc.* **1995**, *117*, 2520.

40 W.-P. Yip, W.-Y. Yu, N. Zhu, C.-M. Che, *J. Am. Chem. Soc.* **2005**, *127*, 14239.

41 J. T. Groves, T. E. Nemo, *J. Am. Chem. Soc.* **1983**, *105*, 5786.

42 J. M. Mayer, *Acc. Chem. Res.* **1998**, *31*, 441.

43 F. R. Mayo, *Acc. Chem. Res.* **1968**, *1*, 193.

44 N. End, A. Pfaltz, *Chem. Commun.* **1998**, 589.

45 C. Ho, W.-H. Leung, C.-M. Che, *J. Chem. Soc., Dalton Trans.* **1991**, 2933.

46 M. Bonchio, S. Campestrini, V. Conte, F. Di Furia, S. Moro, *Tetrahedron* **1995**, *51*, 12363.

47 a) A. Chellamani, P. Kulanthaipandi, S. Rajagopal, *J. Org. Chem.* **1999**, *64*, 2232. b) M. E. Gonzalez-Nunez, R. Mello, J. Royo, G. Asensio, I. Monzo, F. Tomas, J. G. Lopez, F. L. Ortiz, *J. Org. Chem.* **2004**, *69*, 9090.

48 a) C.-M. Che, W.-T. Tang, W.-O. Lee, K.-Y. Wong, T.-C. Lau, *J. Chem. Soc., Dalton Trans.* **1992**, 1551. b) W.-H. Fung, W.-Y. Yu, C.-M. Che, *J. Org. Chem.* **1998**, *63*, 2873.

49 B. B. Wentzel, P. L. Alsters, M. C. Feiters, R. J. M. Nolte, *J. Org. Chem.* **2004**, *69*, 3453.

50 K. Kaneda, K. Jitsukawa, T. Itoh, S. Teranishi, *J. Org. Chem.* **1980**, *45*, 3004.

51 A. J. Appleton, S. Evans, J. R. L. Smith, *J. Chem. Soc., Perkin Trans. 2* **1996**, 281.

52 J. Bernadou, B. Meunier, *Chem. Commun.* **1998**, 2167.

53 a) N. J. Kerrigan, I. J. Langan, C. T. Dalton, A. M. Daly, C. Bousuet, D. G. Gilheany, *Tetrahedron Lett.* **2002**, *43*, 2107. b) J. P. Collman, L. Zeng, J. I. Brauman, *Inorg. Chem.* **2004**, *43*, 2672.

54 a) C.-M. Che, K.-Y. Wong, C.-K. Poon, *Inorg. Chem.* **1985**, *24*, 1797. b) C.-M. Che, T.-F. Lai, K.-Y. Wong, *Inorg. Chem.* **1987**, *26*, 2289. c) M. M. Taqui Khan, C. Sreelatha, S. A. Marza, G. Ramachandraiah, S. H. R. Abdi, *Inorg. Chim. Acta* **1988**, *154*, 103. d) C.-M. Che, C.-K. Li, W.-T. Tang, W.-Y. Yu, *J. Chem. Soc., Dalton Trans.* **1992**, 3153. e) C.-M. Che, W.-Y. Yu, P.-M. Chan, W.-C. Cheng, S.-M. Peng, K. C. Lau, W.-K. Li,

J. Am. Chem. Soc. **2000**, *122*, 11380.
55 J. B. Fenn, *Angew. Chem., Int. Ed.* **2003**, *42*, 3871.
56 D. Feichtinger, D. A. Plattner, *J. Chem. Soc., Perkin Trans. 2* **2000**, 1023.
57 O. Kennard, J. C. Speakman, J. H. D. Donnay, *Acta Crystallogr.* **1967**, *22*, 445.
58 *International Tables for X-ray Crystallography*, ed. by J. A. Ibers, W. C. Hamilton, Kynoch Press, Birmingham, U.K., **1974**, Vol. IV.
59 *teXsan, Crystal Structure Analysis Package*, Molecular Structure Corporation, **1999**.